Asteroseismology of OB stars in the space era

What did we learn from the observations?

Peter De Cat

Royal Observatory of Belgium, Ringlaan 3, B-1180 Brussels, Belgium

... a very incomplete point of view

Convective core
Radiative envelope

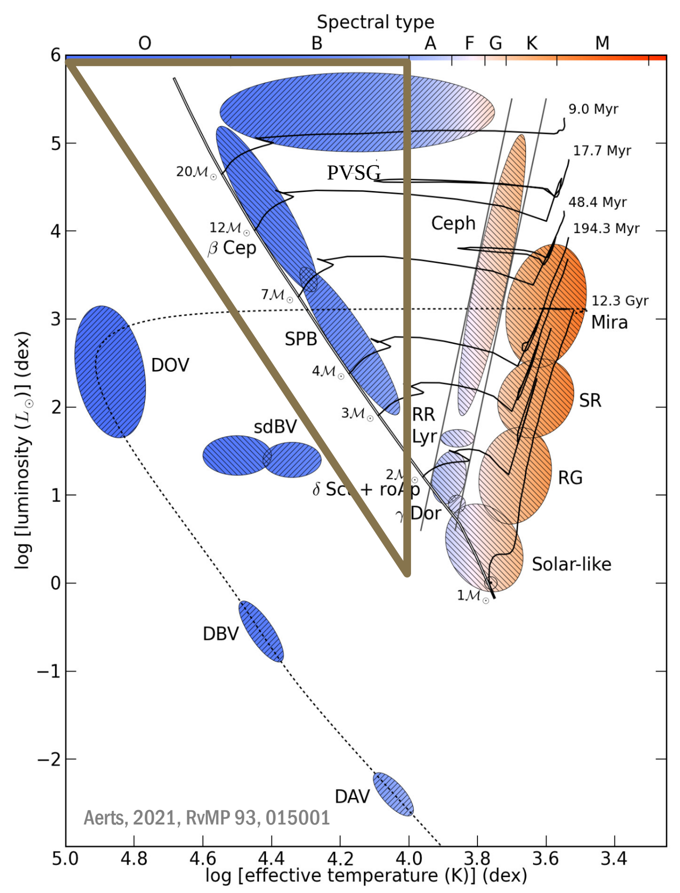

Aerts, 2021, RvMP 93, 015001

→ **β Cephei stars** (βCep)
- ➢ Low order p and g modes with periods of few hours

→ **Slowly Pulsating B stars** (SPB)
- ➢ High order g modes with periods of several hours to few days

Hybrids?

→ **Periodic Variable Supergiants** (PVSG)
- ➢ g modes with periods of order of 10 to 100 days

→ Be stars (Be)
- ➢ Rotational modulation and/or Pulsations?

→ Maia variables

Excitation mechanisms at play
- ➢ Opacity mechanism operating in Z bump

Asteroseismic requirements and tools

→ Time series

→ Observed pulsation modes

- Frequency f → Frequency analysis
- Degree ℓ
- Azimuthal number m

} → Mode identification

⇓

Modelling

Mode identification
- * Multicolour photometry: method of photometric amplitude ratios and frequency shifts (Dupret et al., 2003, A&A 398, 677)
- * High-resolution spectroscopy: moment method (Aerts, 1992, A&A 266, 294; Briquet & Aerts, 2003, A&A 398, 687)
  fourier parameter fit method (Zima, 2006, A&A 455, 227)

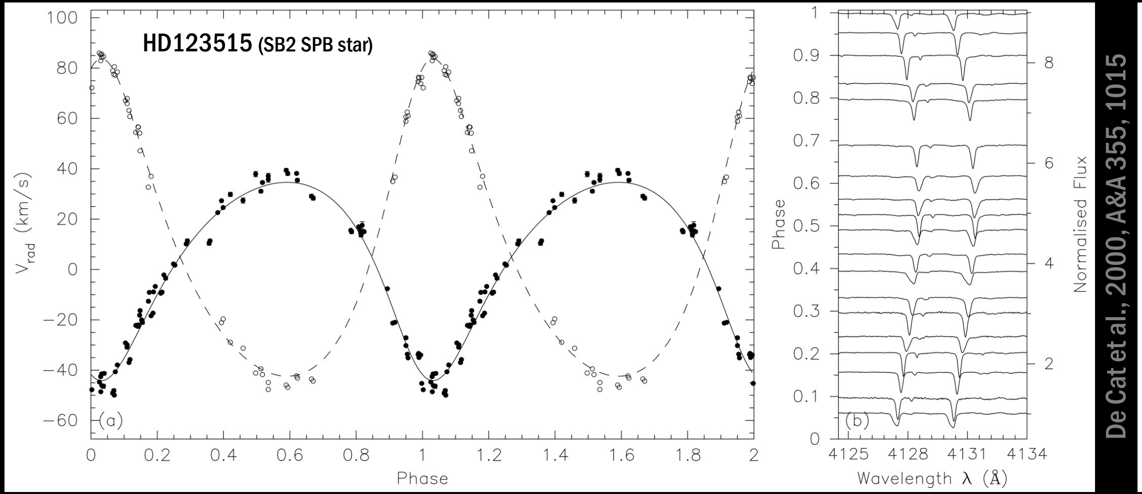

De Cat et al., 2000, A&A 355, 1015

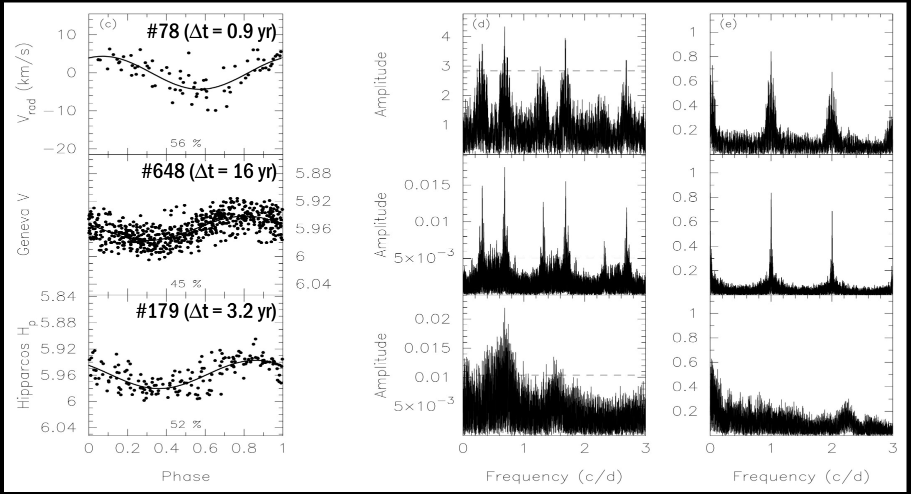

Asteroseismic requirements and tools

→ Time series

→ Observed pulsation modes

- Frequency f ⟶ Frequency analysis
- Degree ℓ
- Azimuthal number m

Degree ℓ and azimuthal number m ⟶ Mode identification

* Multicolour photometry: method of photometric amplitude ratios and frequency shifts (Dupret et al., 2003, A&A 398, 677)

* High-resolution spectroscopy: moment method (Aerts, 1992, A&A 266, 294; Briquet & Aerts, 2003, A&A 398, 687)

fourier parameter fit method (Zima, 2006, A&A 455, 227)

⇓

Modelling

Asteroseismic requirements and tools

→ Time series

→ Observed pulsation modes

➢ Frequency f → Frequency analysis

➢ Degree ℓ

➢ Azimuthal number m

} → Mode identification

* Multicolour photometry: method of photometric amplitude ratios and frequency shifts (Dupret et al., 2003, A&A 398, 677)
* High-resolution spectroscopy: moment method (Aerts, 1992, A&A 266, 294; Briquet & Aerts, 2003, A&A 398, 687)
  fourier parameter fit method (Zima, 2006, A&A 455, 227)

⇓

Modelling

→ Present day asteroseismic diagnostics

➢ Rotational multiplets

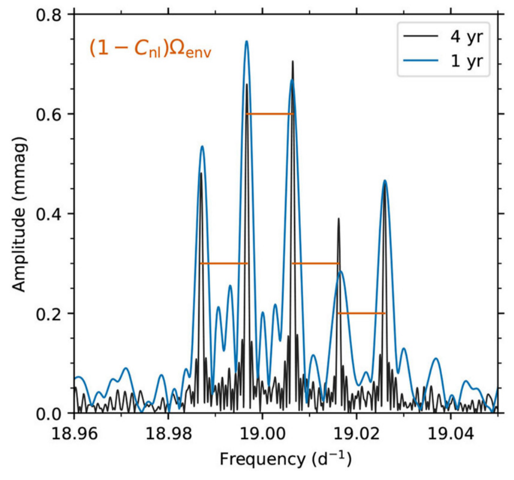

Bowman, 2020, FrASS 7, 70

➢ g mode period spacing patterns (asymptotic regime)

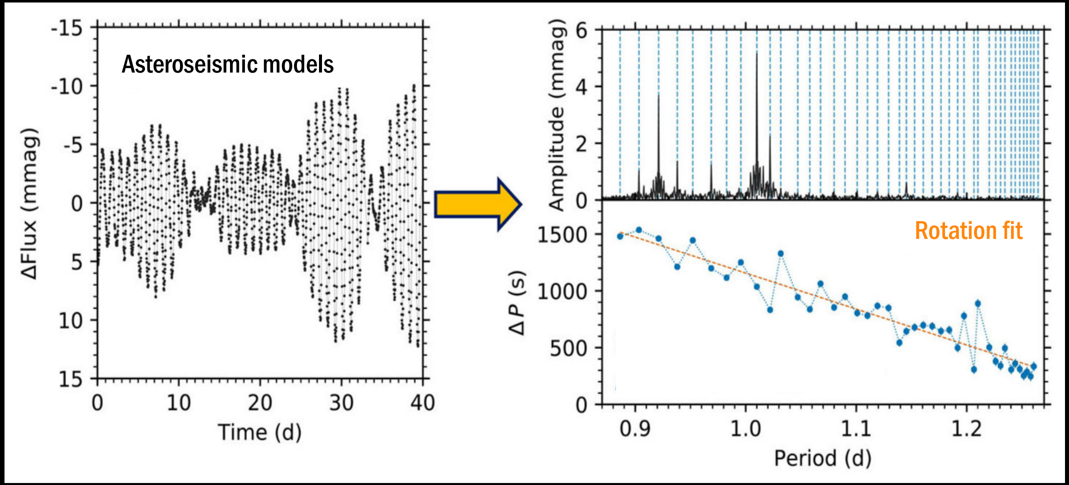

Bowman, 2020, FrASS 7, 70

Asteroseismic requirements and tools

→ Time series

→ Observed pulsation modes

- Frequency f → Frequency analysis
- Degree ℓ
- Azimuthal number m

Degree ℓ and azimuthal number m → Mode identification

* Multicolour photometry: method of photometric amplitude ratios and frequency shifts (Dupret et al., 2003, A&A 398, 677)

* High-resolution spectroscopy: moment method (Aerts, 1992, A&A 266, 294; Briquet & Aerts, 2003, A&A 398, 687)

fourier parameter fit method (Zima, 2006, A&A 455, 227)

→ Present day asteroseismic diagnostics

- Rotational multiplets

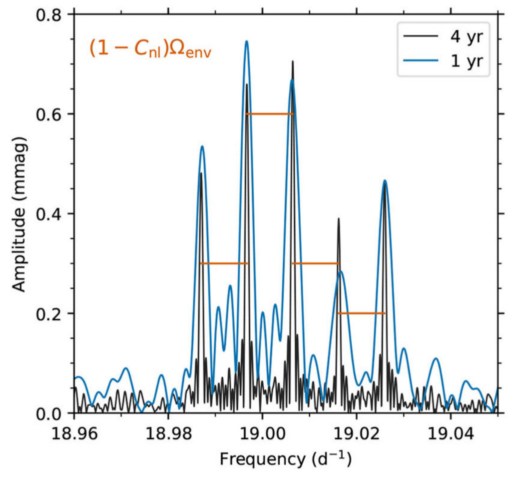

Bowman, 2020, FrASS 7, 70

- g mode period spacing patterns (asymptotic regime)

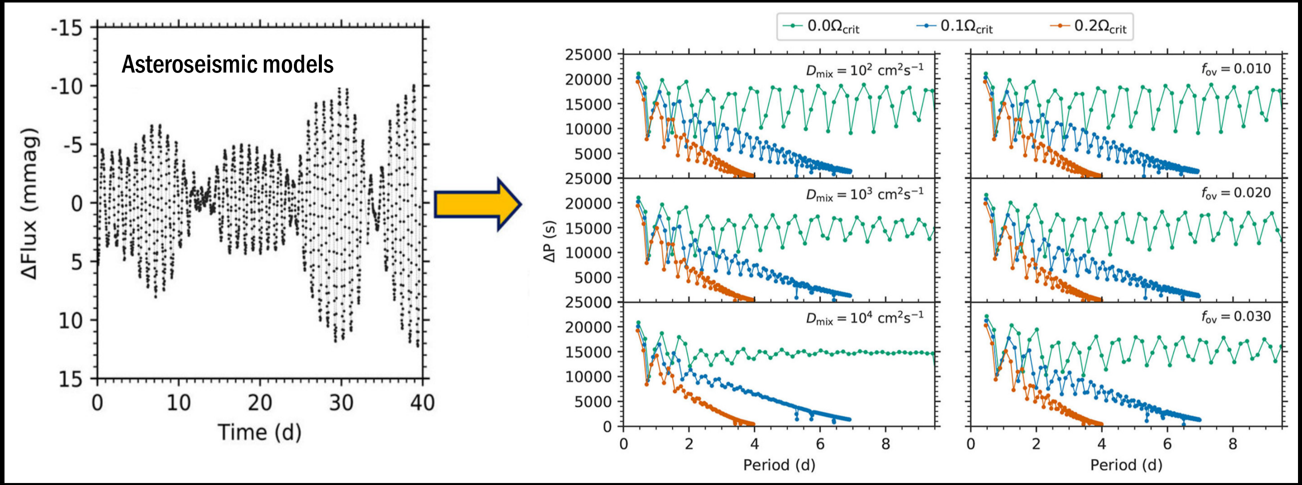

Bowman, 2020, FrASS 7, 70

Magnetic fields

Fossil field

→ Effects of magnetic field on asteroseismic diagnostics of pulsating stars

- ➢ Magnetic multiplets
  (Shibahashi & Aerts, 2000, ApJ 531, L143)
- ➢ Period spacings
  (Prat et al., 2020, A&A 636, A100)
- ➢ Inhibition of mixing ⇒ no overshooting
  (Briquet et al., 2016, A&A 587, A126)

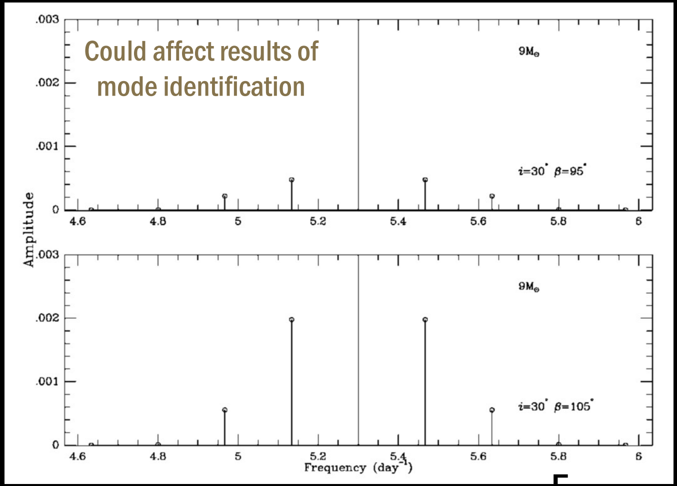
Could affect results of mode identification

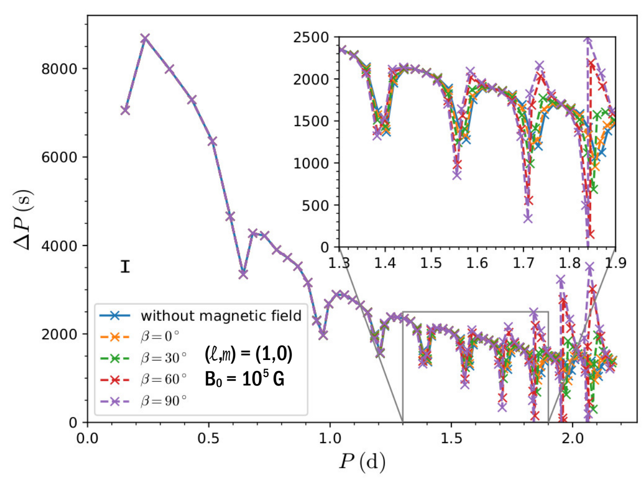

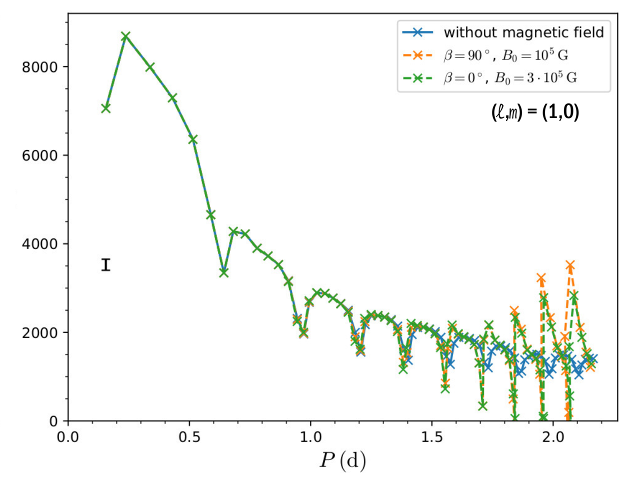

Magneto-asteroseismology

✔	Ground-based	β Cep	(Shibahashi & Aerts, 2000, ApJ 531, L143)
		ζ Cas	(Briquet et al., 2016, A&A 587, A126)
		V2052 Oph	(Briquet et al., 2012, MNRAS 427, 483)
✔	CoRoT	HD43317	(Buysschaert et al., 2018, A&A 616, A148)
✔	K2	ι Lib	(Buysschaert et al., 2018, SF2A Conf., 369)

Talk Neiner: “Magneto-asteroseismology of hot stars” and others

Opacities

→ θ Ophiuchi (Walczak et al., 2019, MNRAS 485, 3544)

- ➢ Known βCep pulsator with 7 pulsation frequencies **Hybrid pulsator**
- ➢ Triple system:
  - ✔ θ Oph Aa: massive B2IV star
  - ✔ θ Oph Ab: low-mass star ($M < 1 M_{\odot}$)
  - ✔ θ Oph B: massive B5 star

} 56.71 days (θ Oph Aa, Ab)

} ~ 14 years

Driving

Damping

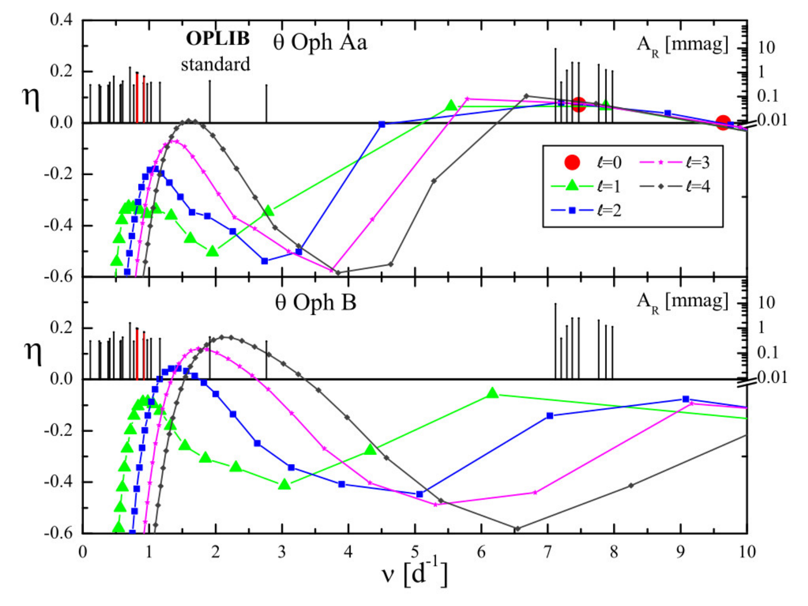

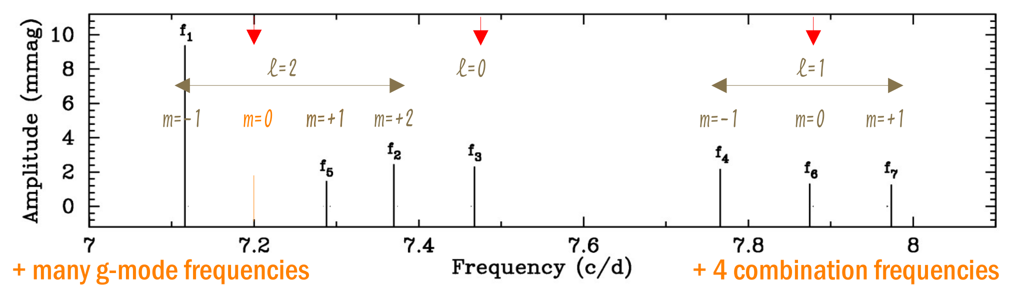

\+ many g-mode frequencies

\+ 4 combination frequencies

BRITE photometry (2014 UBr; 2016+2017 UBr, BHr, BAb, BLb)
SMEI photometry (2003-2010)

- ➢ Complex asteroseismology
  - ✔ Fitting centroid frequencies
  - ✔ Getting the mode instability in the observed frequency range
  - ✔ Reproduce the emperical value of *f* (ratio of the relative bolometric flux to the relative radial displacement)

(cf. Talk Daszyńska-Daszkiewicz)

Opacities

→ θ Ophiuchi (Walczak et al., 2019, MNRAS 485, 3544)

- Known βCep pulsator with 7 pulsation frequencies — Hybrid pulsator
- Triple system:
  - ✔ θ Oph Aa: massive B2IV star
  - ✔ θ Oph Ab: low-mass star ($M < 1\ M_\odot$)
  - ✔ θ Oph B: massive B5 star

θ Oph Aa + θ Oph Ab: 56.71 days

θ Oph A + θ Oph B: ~ 14 years

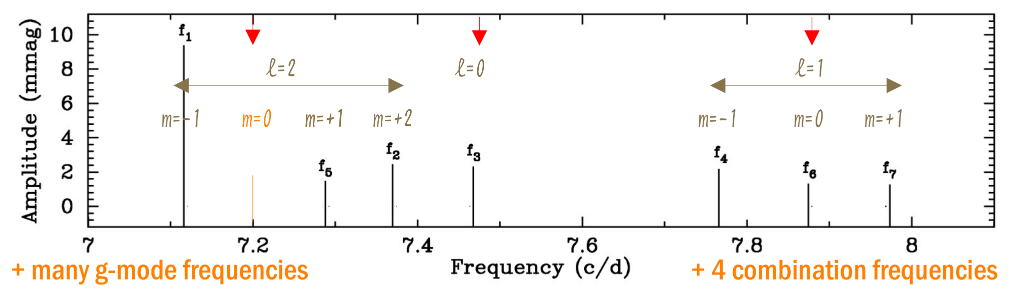

+ many g-mode frequencies

+ 4 combination frequencies

BRITE photometry (2014 UBr; 2016+2017 UBr, BHr, BAb, BLb)
SMEI photometry (2003-2010)

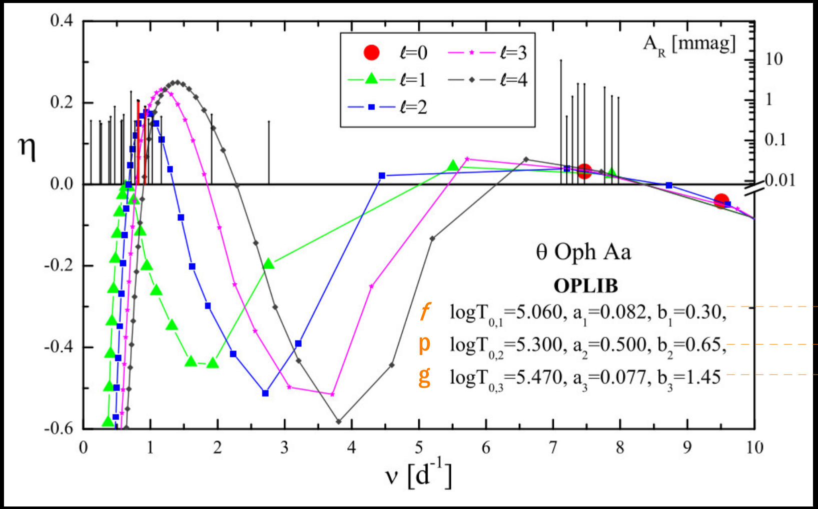

Kurucz bump

Z-bump

Ni

- Complex asteroseismology
  - ✔ Fitting centroid frequencies
  - ✔ Getting the mode instability in the observed frequency range
  - ✔ Reproduce the emperical value of *f* (ratio of the relative bolometric flux to the relative radial displacement)

(cf. Talk Daszyńska-Daszkiewicz)

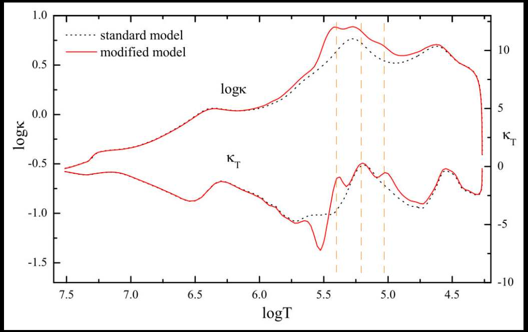

Opacity increase needed to excite g-modes
(θ Oph Aa)

Opacities

→ θ Ophiuchi (Walczak et al., 2019, MNRAS 485, 3544)

- Known βCep pulsator with 7 pulsation frequencies — Hybrid pulsator
- Triple system:
  - ✔ θ Oph Aa: massive B2IV star
  - ✔ θ Oph Ab: low-mass star (M < 1 $M_\odot$)
  - ✔ θ Oph B: massive B5 star

} 56.71 days (θ Oph Aa + θ Oph Ab)

} ~ 14 years

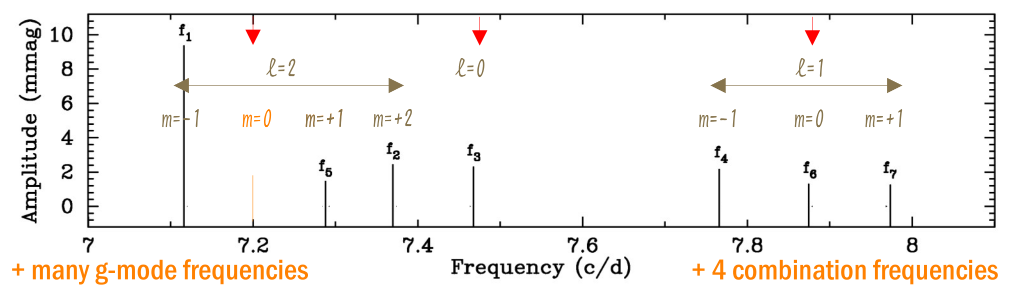

+ many g-mode frequencies

+ 4 combination frequencies

BRITE photometry (2014 UBr; 2016+2017 UBr, BHr, BAb, BLb)
SMEI photometry (2003-2010)

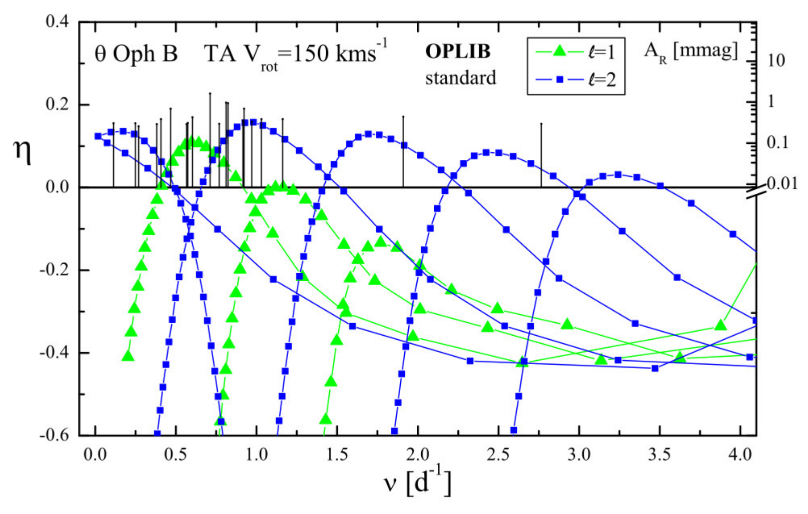

- Complex asteroseismology
  - ✔ Fitting centroid frequencies
  - ✔ Getting the mode instability in the observed frequency range
  - ✔ Reproduce the emperical value of *f* (ratio of the relative bolometric flux to the relative radial displacement)

Fast rotation needed to excite g-modes

(θ Oph B)

Opacity increase needed to excite g-modes

(θ Oph Aa)

Opacities

- → θ Ophiuchi (Walczak et al., 2019, MNRAS 485, 3544)
- → β Centauri (Pigulski et al., 2016, A&A 588, A55)
  - ➢ Triple system:
    - ✔ β Cen Aa: early B-type star (M = 12.02(13) $M_\odot$), faster rotator (v_{rot} = 200-250 km s^{-1})
    - ✔ β Cen Ab: early B-type star (M = 10.58(18) $M_\odot$), slower rotator (v_{rot} = 70-120 km s^{-1}), magnetic
    - ✔ β Cen B: distant, mid B-type star
  - ➢ 8 g-modes, 9 p-modes, and 2 combination frequencies

357 days
e=0.81
resolved

125-220 years

BRITE photometry (2014, 146d, UBr, BTr, BAb, BLb)
BRITE photometry (2014, 27d, BLb)
BRITE photometry (2014, 6d, BTr)

Ideal to study influence of

Rotation

Magnetic field

Light time effect: attribution to Aa and Ab component inconclusive for most frequencies

If effects rotation taken into account, no need for

Increase opacity
Increase metallicity
Change chemical composition

Coeval models

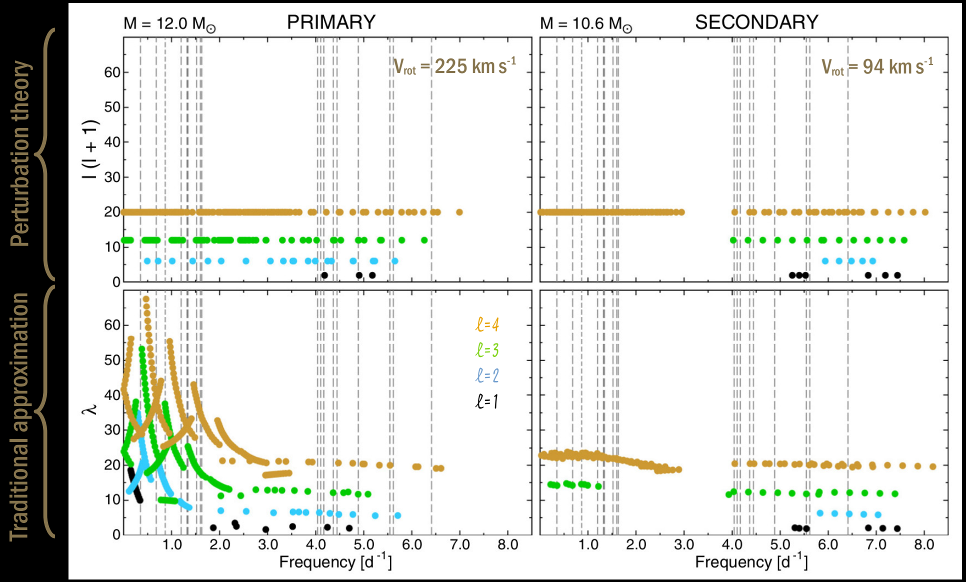

Interior mixing profile

→ Pedersen et al., 2021, NatAs 5, 715

- Sample of 26 SPB stars showing period spacings patterns from dipole g-modes (~4% of all B stars in the nominal Kepler field of view)
- Asteroseismic modelling with eight different interior mixing profiles $D_{mix}(r)$ each having three regions (convective core $D_{conv}(r)$, core boundary layer $D_{cbl}(r)$, radiative envelope $D_{env}(r)$)

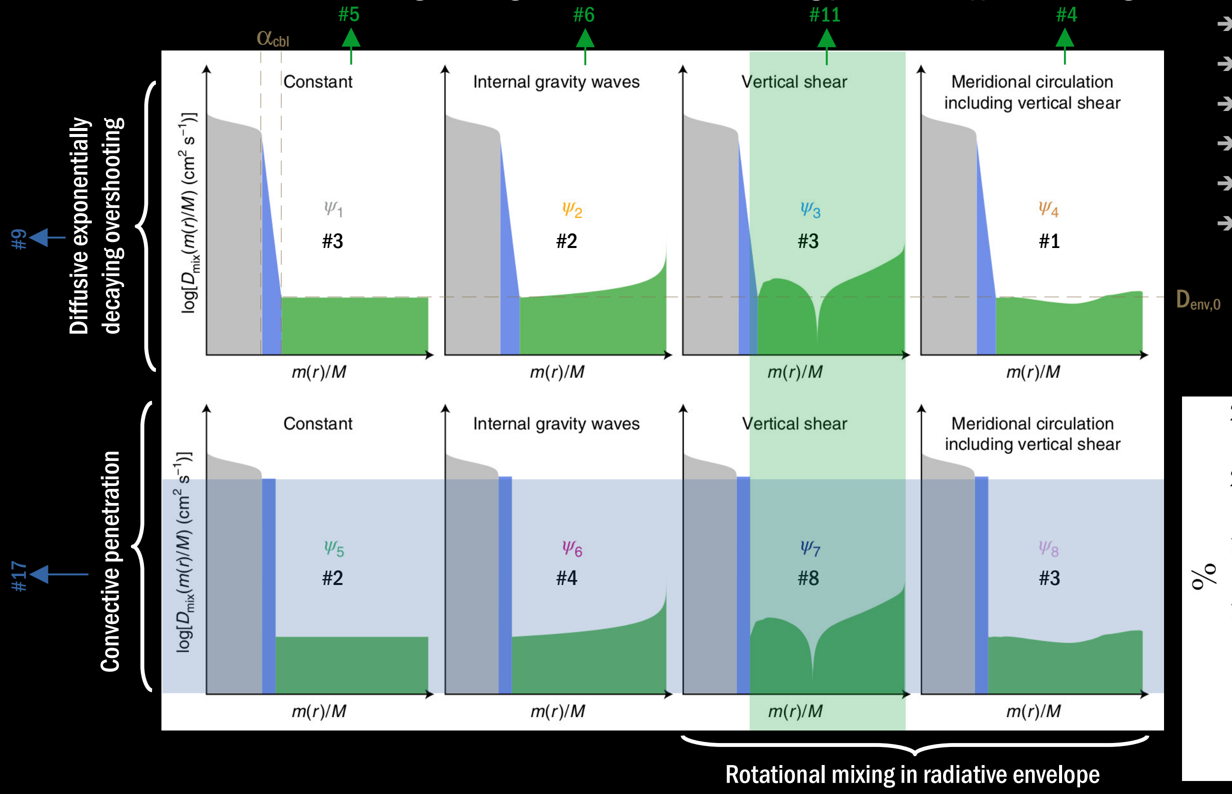

➔	M_{ini}	initial mass
➔	Z	metal mass fraction
➔	X_c/X_{ini}	hydrogen mass fraction in fully mixed convective core/inital hydrogen mass fraction
➔	Ω_{rot}	interior rotation frequency
➔	α_{cbl}	length scale connected with the size of the core boundary layer
➔	$D_{env,0}$	level of mixing at bottom of radiative envelope

Majority for convective penetration (55%)
vertical shear (39%)

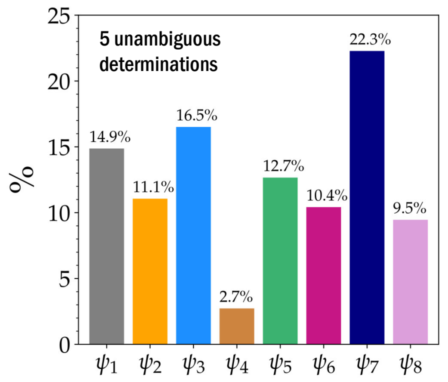

Pedersen, 2022, ApJ 930, 94

➔ Expected helium core masses at end of main-sequence evolution:
* underestimated without mixing
* increase with initial stellar mass
* heavily influenced by amount of envelope mixing

cf. Kaiser et al, 2020, MNRAS 496, 1967
Johnston, 2021, A&A 655, A29

Interior rotation profile

→ **HD201433** (Kallinger et al., 2017, A&A 603, A13)

BRITE photometry (6 seasons in 2013-2019; 156 days; BTr, BIb; cadence 0.338 min)
SMEI photometry (8 years; 101.6 min)
Radial velocites (96 years)

- ➢ Single-lined spectroscopic triple system:
  - ✔ B9V star (suspected SPB star; close to the cool border of instability strip) with two low mass companions
  - ✔ 3.3 days
  - ✔ 154 days
- ➢ Frequency analysis BTr data
  - ✔ 9 statisticaly significant closely separated doublets (ℓ=1 modes with m=±1) (red squares)
  - ✔ 4 additional independent frequencies
  - ✔ 7 combination frequencies

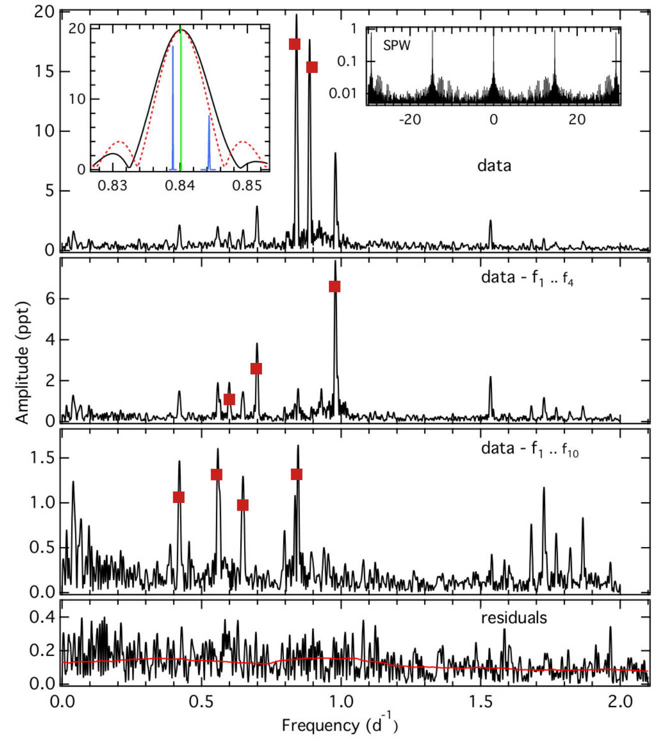

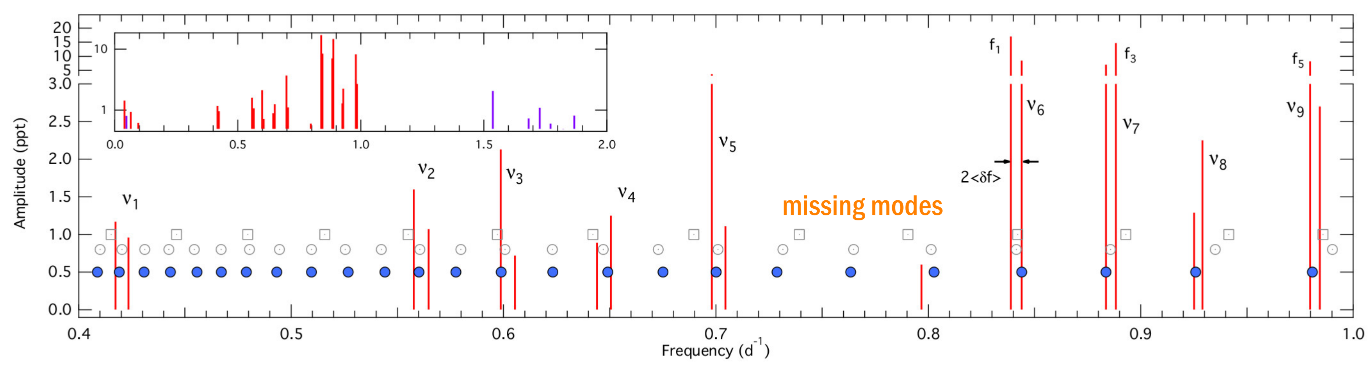

Interior rotation profile

→ **HD201433** (Kallinger et al., 2017, A&A 603, A13)

- Single-lined spectroscopic triple system:
  - ✔ B9V star (suspected SPB star; close to the cool border of instability strip) with two low mass companions
  - ✔ 3.3 days
  - ✔ 154 days
- Frequency analysis BTr data
- Frequency analysis SMEI data
  - ✔ Confirmation 3 closely separated triplets of ℓ=1 modes
  - ✔ Evidence for amplitude changes (mode lifetime of 680(110) days)

BRITE photometry (6 seasons in 2013-2019; 156 days; BTr, Blb; cadence 0.338 min)
SMEI photometry (8 years; 101.6 min)
Radial velocites (96 years)

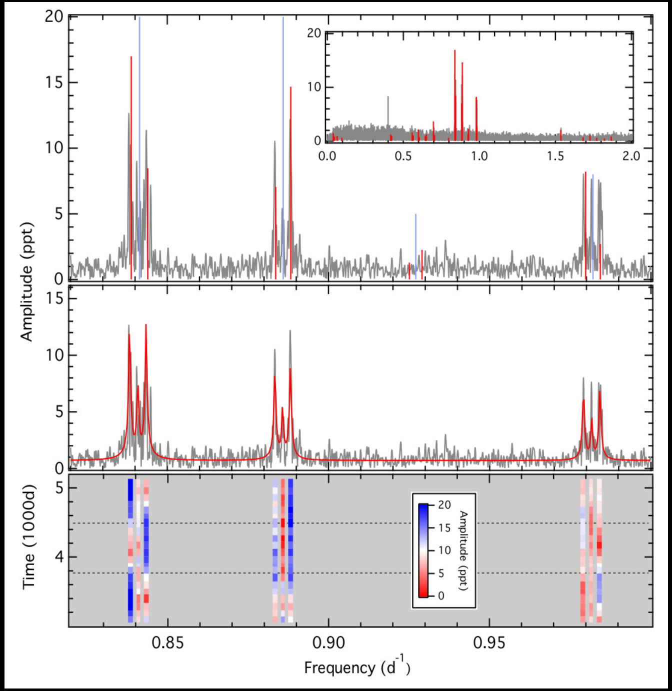

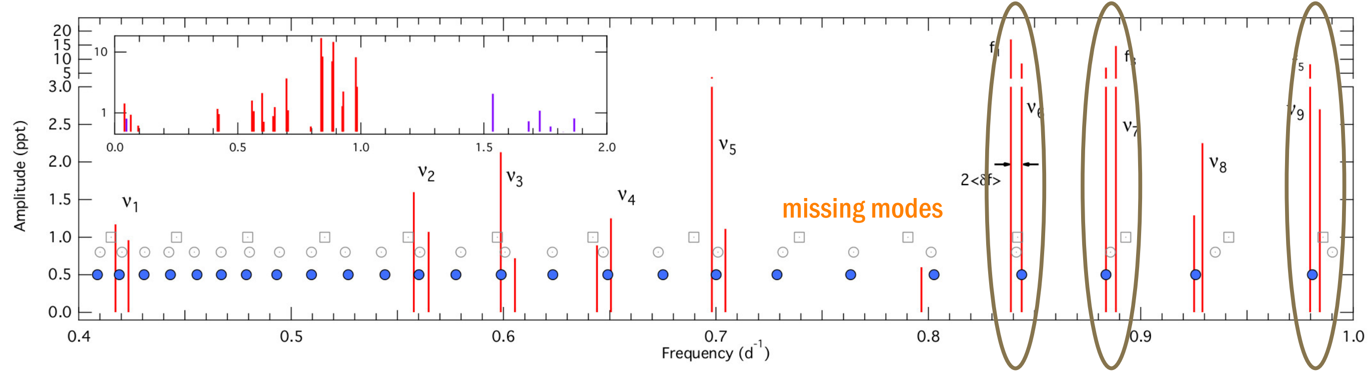

Interior rotation profile

- **HD201433** (Kallinger et al., 2017, A&A 603, A13)
  - Single-lined spectroscopic triple system:
    - B9V star (suspected SPB star; close to the cool border of instability strip) with two low mass companions
    - 3.3 days
    - 154 days
  - Frequency analysis BTr data
  - Frequency analysis SMEI data
  - Interior rotation profile radiative envelope
    - Slowly and ridigly rotating envelope
    - Thin and significantly more rapidly rotating surface layer
      - Compatible with orbital period of innermost companion

BRITE photometry (6 seasons in 2013-2019; 156 days; BTr, Blb; cadence 0.338 min)
SMEI photometry (8 years; 101.6 min)
Radial velocites (96 years)

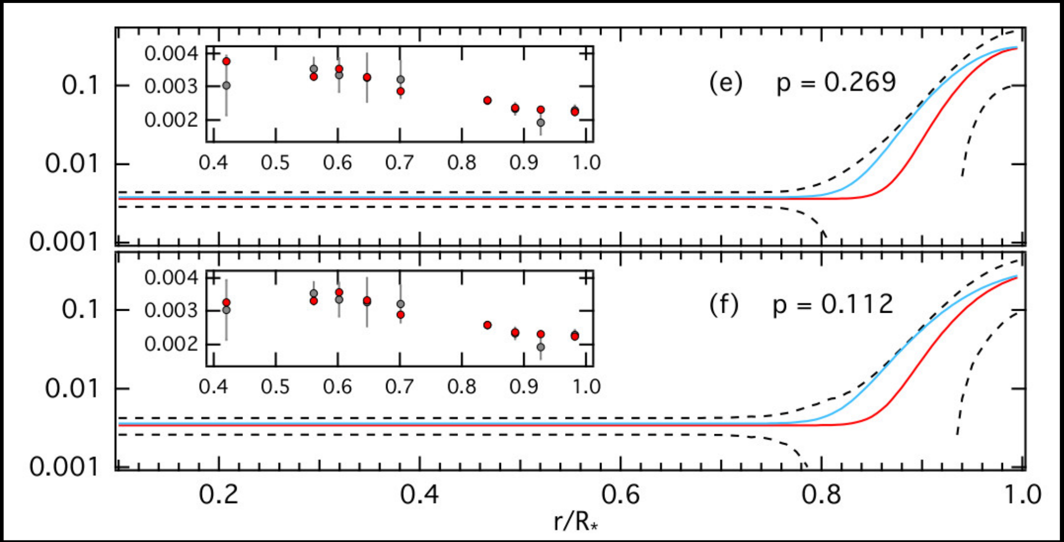

- Pedersen, 2022, ApJ 940, 49
  - Core rotation decreases with age
  - Evidence for angular momentum transport on main-sequence

Tidal forces

→ ι Orionis (Pablo et al., 2017, MNRAS 467, 2494)

- Massive binary
  - ✔ O9 III + B1 III/IV
  - ✔ P_{orb} = 29.13376 days
  - ✔ e = 0.764
- Frequency analysis
  - ✔ 7 frequencies

BRITE photometry (2013 & 2015; 9 months; UBr, BTr, BHr, BAb, BIb)
High-resolution spectra (2025-2016; #11; 1.06-m Ritter Observatory)
Archival radial velocities (Marchenko et al., 2000, MNRAS 317, 333)

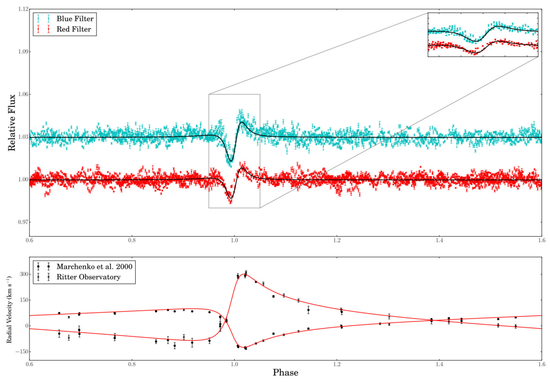

(cf. Talk Kolaczek-Szymańsky)

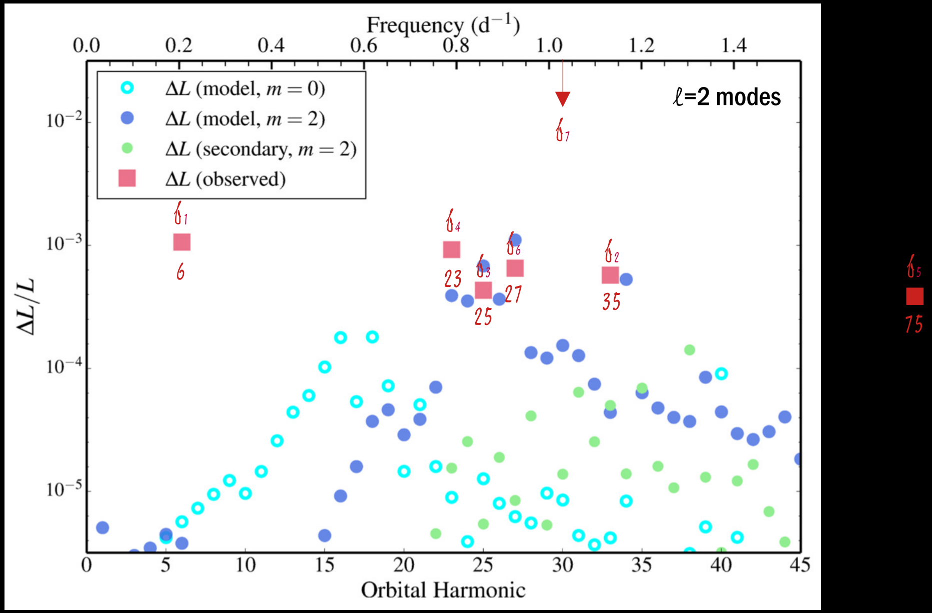

Tidally excited oscillations discovered in O stars

(heartbeat signal at periastron)

→ η Carina (Richardson et al., 2018, MNRAS 475, 5417)

→ ε Lupi (Pablo et al., 2019, MNRAS 488, 64)

Tidal forces

→ π^5 Orionis (Jerzykiewicz et al., 2020, MNRAS 496, 2391)

- ➢ SB1 system and ellipsoidal variable
  - ✔ Two early B-type stars
  - ✔ P_{orb} = 3.70 days
  - ✔ Circularized orbit
  - ✔ Synchronized rotation
- ➢ Frequency analysis
  - ✔ 9 frequencies

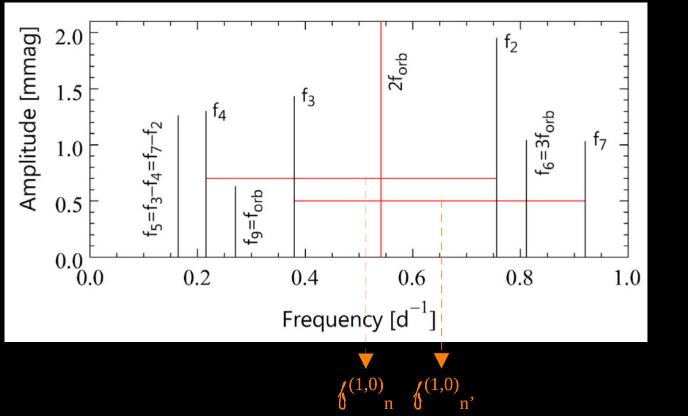

BRITE photometry (6 seasons in 2013-2019; UBr, BTr, BHr, BAb, BLb)

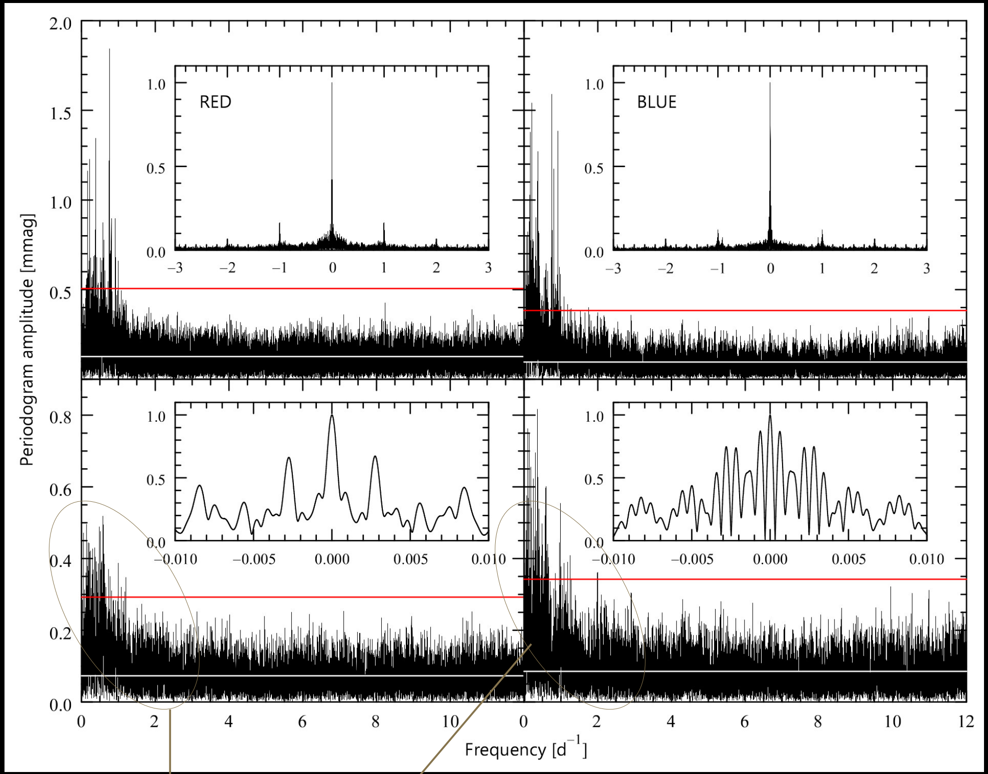

Self excited (ℓ,m)=(1,0) g-modes in primary that are distored by equilibrium tide

(if axis of pulsating component is tilted)

Red noise excess at low frequencies

Stochastic Low-Frequency Variability (SLFV)

→ Observations of SLFV (red noise excess at low frequencies)

- ✔ Blomme et al., 2011, A&A 533, A4 → HD46223, HD46150 & HD4696 (O stars)

CoRoT photometry

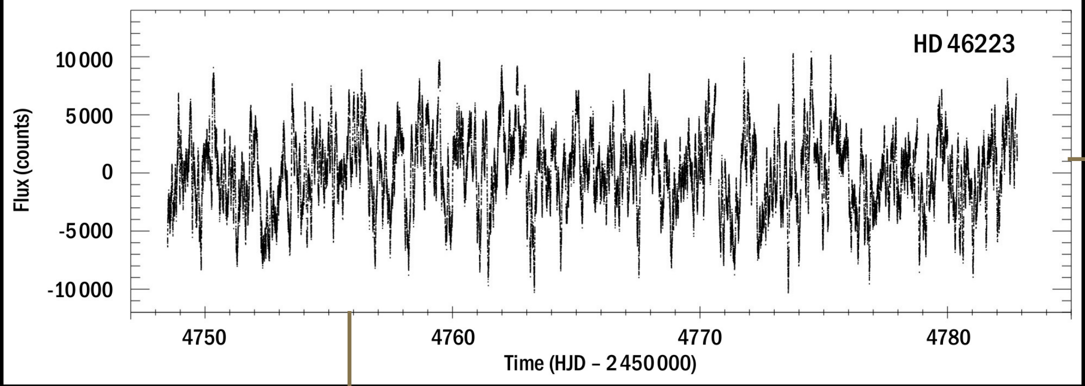

Time-dependent frequency analysis (sliding window)

Short-lived variability

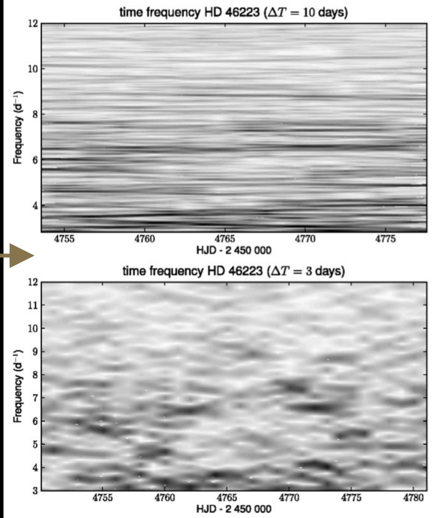

Stochastic excitation

Lomb-Scargle periodogram

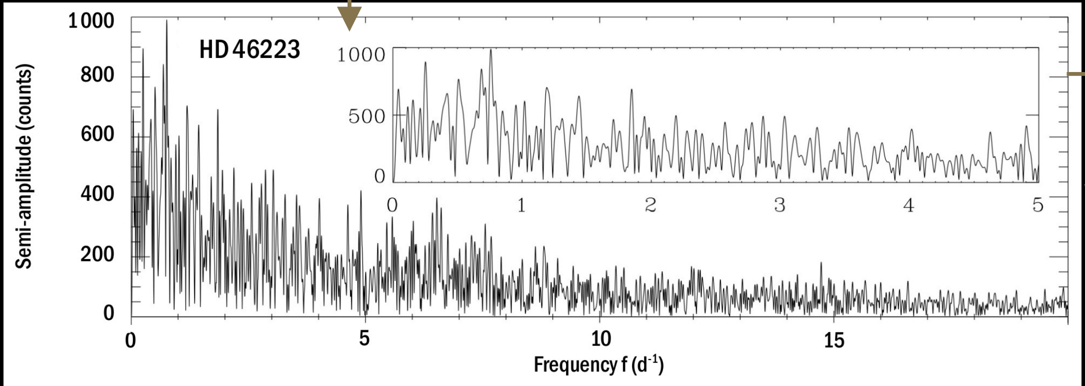

Semi-Lorentzian function

$$\alpha(f) = \frac{\alpha_0}{1 + (2\pi\tau_{char} f)^{\gamma}}$$

with

- α_0 amplitude as f → 0
- τ_{char} characteristic timescale on which red noise is correlated
- γ steepness of amplitude spectrum

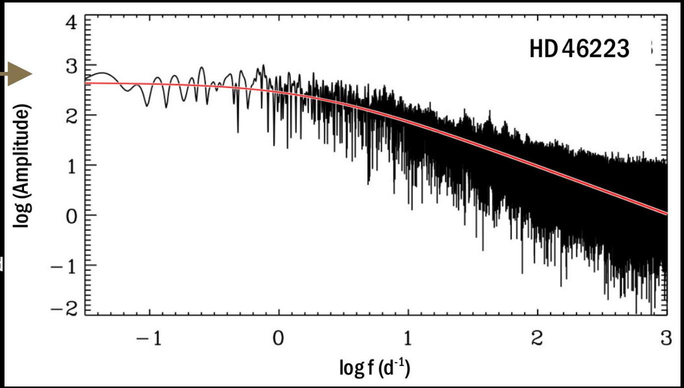

Stochastic Low-Frequency Variability (SLFV)

→ Observations of SLFV (red noise excess at low frequencies)

✔	Blomme et al., 2011, A&A 533, A4	→ HD46223, HD46150 & HD4696 (O stars)	CoRoT
✔	Tkachenko et al., 2014, MNRAS 438, 3093	→ primary of massive binary V380 Cyg (B star)	Kepler + spectra
✔	Aerts et al., 2017, A&A 602, A32	→ HD188209 (O9.5 Iab blue supergiant)	Kepler + spectra
✔	Simón-Díaz et al., 2018, A&A 612, A40	→ HD2905 (early-B supergiant)	spectra
✔	Ramiaramanantsoa et al., 2018, MNRAS 480, 972	→ V973 Scorpii (O-type supergiant)	BRITE
✔	Bowman et al., 2019, A&A 621, A135	→ 35 OBAF stars	CoRoT
✔	Bowman et al., 2019, NatAs 3, 760	→ 114 ecliptic OB stars & 53 LMC OB stars	K2 + TESS
✔	Dorn-Wallenstein et al., 2019, AJ 878, 155	→ 6 LMC yellow supergiants & 2 LMC luminous blue variables	TESS
✔	Bowman et al., 2020, A&A 640, A36	→ 70 OB stars	TESS + spectra
✔	Dorn-Wallenstein et al., 2020, AJ 902, 24	→ 28 LMC yellow supergiants & 48 Galactic red supergiants	TESS
✔	Rauw et al., 2019, A&A 621, A15	→ HD149404 (massive post-Roche Lobe overflow system)	BRITE
✔	Nazé et al., 2021, MNRAS 502, 5038	→ 26 Wolf-Rayet stars & 8 luminous blue variables	TESS
✔	Lenoir-Craig et al., 2022, AJ 925, 79	→ 50 Galactic Wolf-Rayet stars	BRITE, TESS, MOST
✔	Elliot et al., 2022, MNRAS 509, 4246	→ P Cygni (luminous blue variable)	BRITE
✔	Bowman et al., 2022, A&A 668, A134	→ 30 OB stars	CoRoT
✔	Kołaczek-Szymański et al., 2022, A&A 659, A47	→ MACHO 80.7443.1718 (blue supergiant + late O-type dwarf)	TESS
✔	Dorn-Wallenstein et al., 2022, AJ 940, 27	→ 101 LMC and 25 SMC cool supergiants	TESS

Feature observed for many different types of massive stars!

Stochastic Low-Frequency Variability (SLFV)

→ Characterisation of SLFV (red noise excess at low frequencies)

- Amplitude spectrum fitting (frequency domain)
  - ✔ Semi-Lorentzian function

α_0	characteristic amplitude as frequency → 0
$\tau_{char} = 1/\nu_{char}$	characteristic timescale on which red noise is correlated
γ	steepness of amplitude spectrum
α_w	frequency independent noise term (white noise)

- Lenoir-Craig et al., 2022, AJ 925, 79 → 50 Galactic Wolf-Rayet stars BRITE (#4), TESS (#49), MOST (#6)
  - ✔ Correlations with stellar and wind characteristics

Stochastic Low-Frequency Variability (SLFV)

→ **Characterisation of SLFV** (red noise excess at low frequencies)

- Amplitude spectrum fitting (frequency domain)
  - ✔ Semi-Lorentzian function
    - ➔ α_0 characteristic amplitude as frequency ⟶ 0
    - ➔ $\tau_{char} = 1/\nu_{char}$ characteristic timescale on which
    - ➔ γ steepness of amplitude spectrum
    - ➔ α_w frequency independent noise term
- Lenoir-Craig et al., 2022, AJ 925, 79
  - ✔ Correlations with stellar and wind characteristics
    - ➔ WR stars without signs of H in spectrum

      hotter, more luminous cWRs with denser winds have higher levels of stochastic variability

Wind terminal velocity | Mass loss rate | Stellar temperature | Absolute velocity Smith v band | Stellar radius | Bolometric luminosity

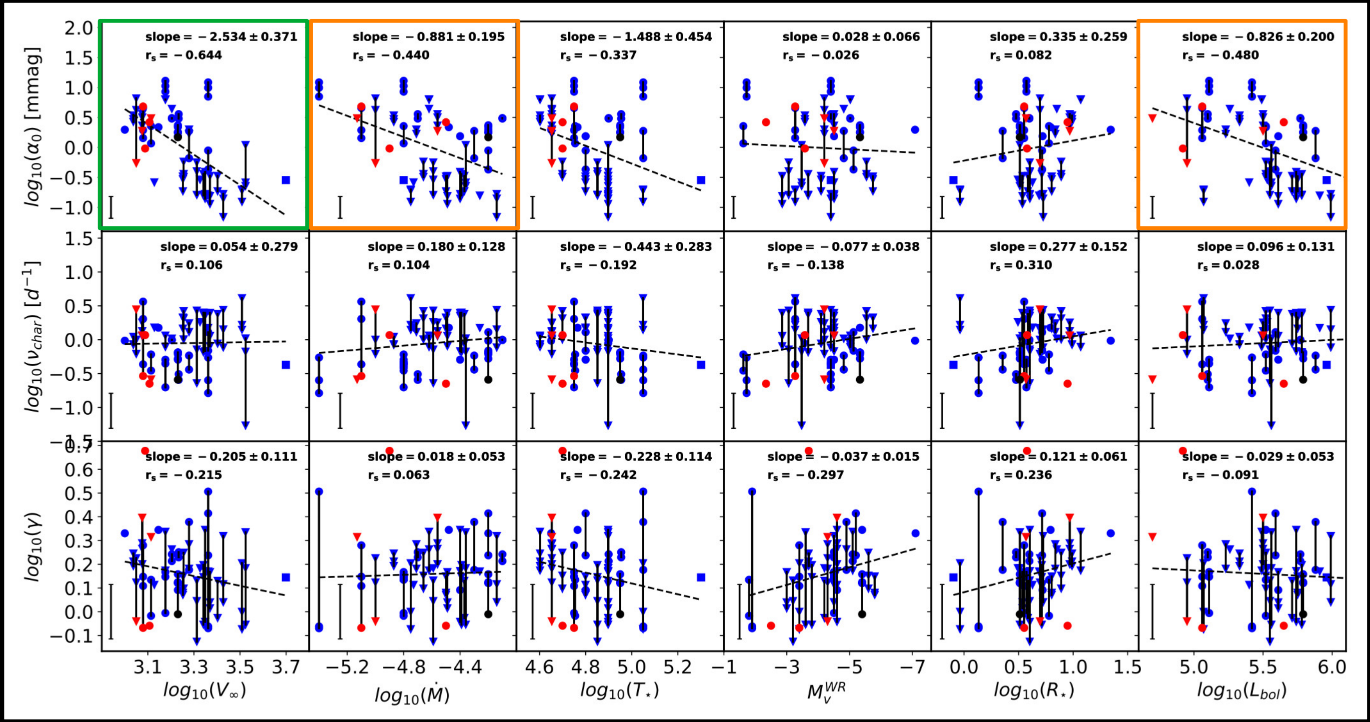

Stochastic Low-Frequency Variability (SLFV)

→ **Characterisation of SLFV** (red noise excess at low frequencies)

- Amplitude spectrum fitting (frequency domain)
  - ✔ Semi-Lorentzian function
    - ➔ α_0 characteristic amplitude as frequency → 0
    - ➔ $\tau_{char} = 1/\nu_{char}$ characteristic timescale on which
    - ➔ γ steepness of amplitude spectrum
    - ➔ α_w frequency independent noise term

- Lenoir-Craig et al., 2022, AJ 925, 79
  - ✔ Correlations with stellar and wind characteristics
    - ➔ WR stars without signs of H in spectrum

      hotter, more luminous cWRs with denser winds have higher levels of stochastic variability
    - ➔ WR stars with signs of H in spectrum

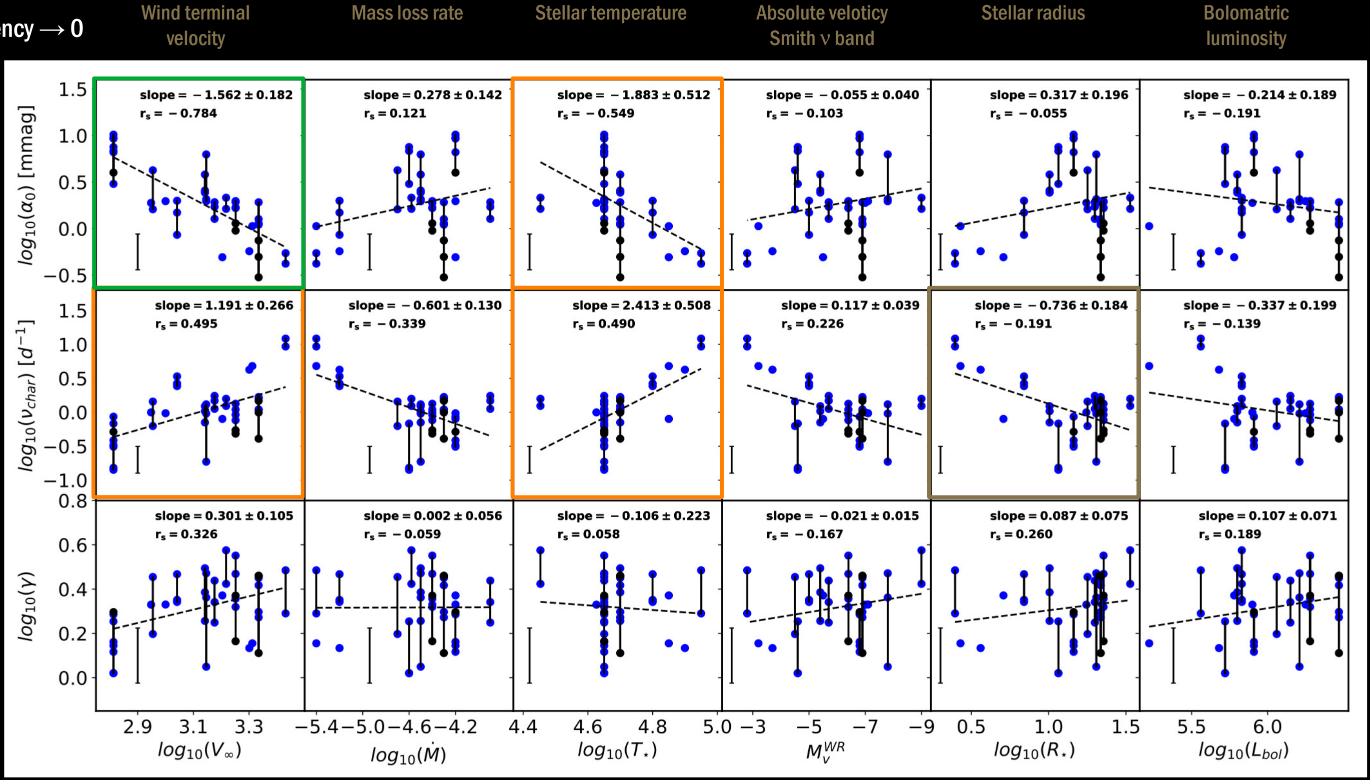

Stars observed at different epochs can have significantly different fitted parameters

Stochastic Low-Frequency Variability (SLFV)

→ Characterisation of SLFV (red noise excess at low frequencies)

- Amplitude spectrum fitting (frequency domain)
  - ✔ Semi-Lorentzian function

➔ α_0	characteristic amplitude as frequency → 0
➔ $\tau_{char} = 1/\nu_{char}$	characteristic timescale on which red noise is correlated
➔ γ	steepness of amplitude spectrum
➔ α_w	frequency independent noise term (white noise)

- Gaussian process regression (time domain)
  - ✔ Damped simple harmonic oscillator

➔ σ_A	characteristic amplitude
➔ $\rho_{char} = 2\pi/\omega_0$	characteristic variability timescale
➔ τ_{damp}	characteristic damping timescale
➔ C_{jitter}	jitter term to emulate uncorrelated noise in the observations
➔ Q	quality factor (more damping if low value)

➢ Lenoir-Craig et al., 2022, AJ 925, 79	→ 50 Galactic Wolf-Rayet stars	BRITE (#4), TESS (#49), MOST (#6)
➢ Bowman et al., 2022, A&A 668, A134	→ 30 OB stars	TESS (#30)

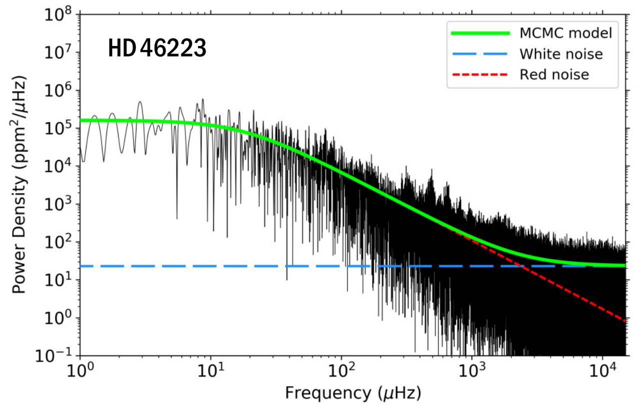

Bowman et al., 2019, A&A 621, A135

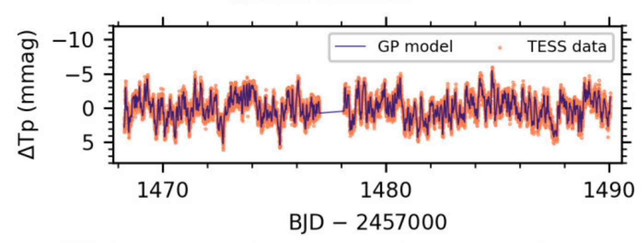

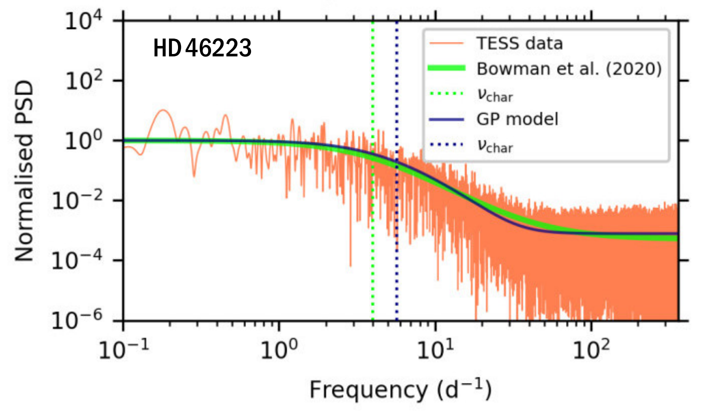

Bowman et al., 2022, A&A 668, A134

Stochastic Low-Frequency Variability (SLFV)

→ Characterisation of SLFV (red noise excess at low frequencies)

- ➢ Amplitude spectrum fitting (frequency domain)
  - ✔ Semi-Lorentzian function
    - ➔ α_0 characteristic amplitude as frequency ⟶ 0
    - ➔ $\tau_{char} = 1/\nu_{char}$ characteristic timescale on which red noise is correlated
    - ➔ γ steepness of amplitude spectrum
    - ➔ α_w frequency independent noise term (white noise)
- ➢ Gaussian process regression (time domain)
  - ✔ Damped simple harmonic oscillator
    - ➔ σ_A characteristic amplitude
    - ➔ $\rho_{char} = 2\pi/\omega_0$ characteristic variability timescale
    - ➔ τ_{damp} characteristic damping timescale
    - ➔ C_{jitter} jitter term to emulate uncorrelated noise in the observations
    - ➔ Q quality factor (more damping if low value)

- ➢ Lenoir-Craig et al., 2022, AJ 925, 79
- ➢ Bowman et al., 2022, A&A 668, A134

“yellow subgroup”:
- Low ν_{char} + high α_0/σ_A + low ν_{damp}
- Higher mass
- More evolved (closer to TAMS)
- Less stochastic (high Q value)

“blue subgroup”:
- High ν_{char} + low α_0/σ_A + high ν_{damp}
- Less evolved (closer to ZAMS)
- More stochastic (low Q values)

ν_{char} probes

Mass

Age

Degree of coherency

Bowman et al., 2022, A&A 668, A134

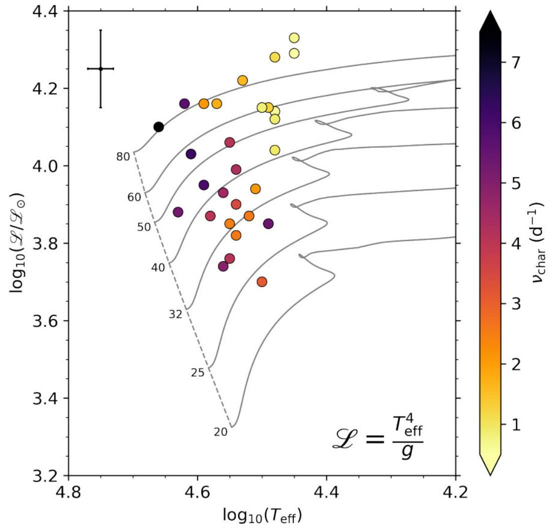

Bowman et al., 2022, A&A 668, A134

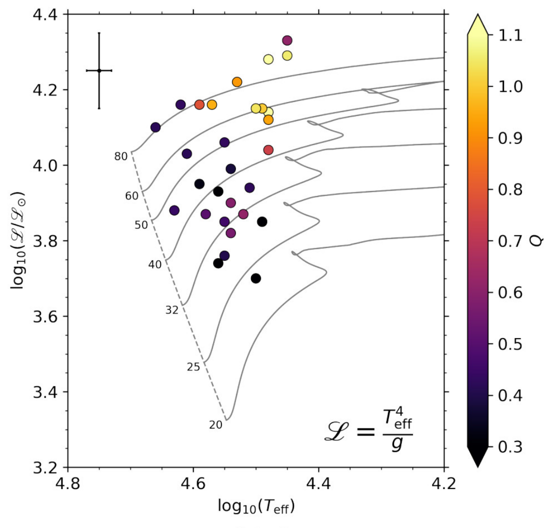

Stochastic Low-Frequency Variability (SLFV)

→ Interpretation of SLFV

- Surface granulations (cf. red giant stars) but ν_{char} order of magnitude smaller than predicted ν_{gran} for majority of stars (Bowman et al., 2019, A&A 621, A135)
- Internal Gravity Waves (IGWs)
  - ✔ Travelling waves that are stochastically excited at the interface of a convective region and a stably stratified zone
    - ➔ turbulent core convection
    - ➔ turbulent pressure fluctuations in subsurface convective zones in outer envelope (Fe-opacity peak converction zone)
  - ✔ Propagate and dissipate within radiative regions
- Wind-driven processes
  - ✔ Clumpy, aspherical, and inhomogeous stellar wind (line deshadowing instability)

No consensus yet…

OB-type stars

Convective core
Radiative envelope

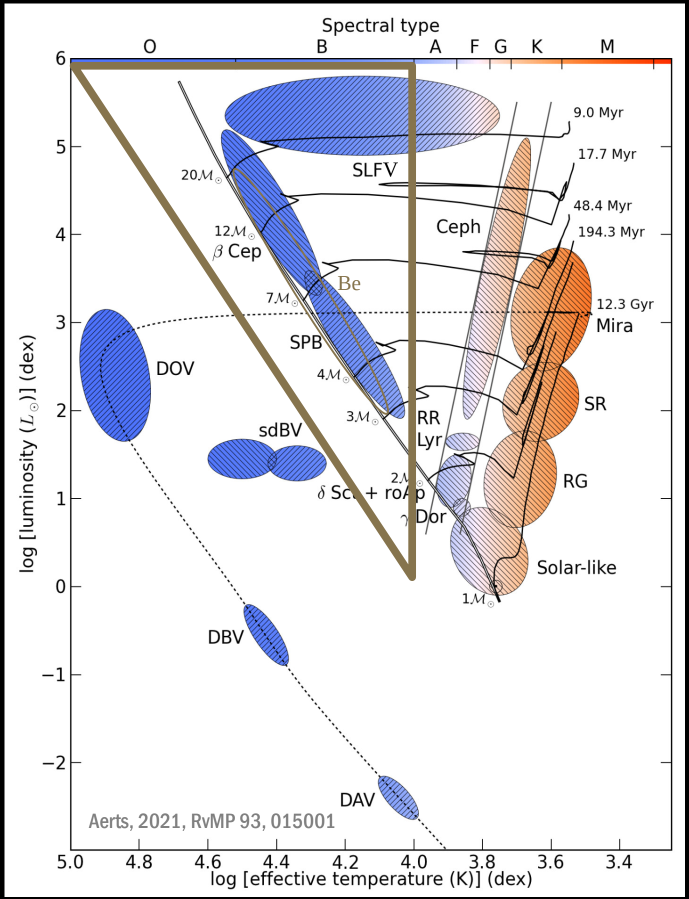

Aerts, 2021, RvMP 93, 015001

- → β Cephei stars (βCep)
  - ➢ Low order p and g modes with periods of few hours
- → Slowly Pulsating B stars (SPB)
  - ➢ High order g modes with periods of several hours to few days

} Hybrids!

- → Stochastic low-frequency variability (SLFV)
  - ➢ α Cygny stars
  - ➢ Fast Yellow Pulsating Supergiants (?)
- → Be stars (Be)
  - ➢ Pulsations (cf. Talk Saio)
- → Maia variables (?)

Excitation mechanisms at play

- ➢ Opacity mechanism operating in Z bump
- ➢ Stochastic excitation
- ➢ Non-linear mode excitation
- ➢ Rotation
- ➢ Tidal excitation

Influencing factors

- ➢ Opacities
- ➢ Interior mixing profile
- ➢ Interior rotation profile
- ➢ Interior temperature profile
- ➢ Tidal forces
- ➢ Magnetic fields
- ➢ Mass loss
- ➢ Stellar wind